Inorg. Chem. **2007**, *46*, 9853–9862

Synthesis and Characterization of Ruthenium and Rhenium Nucleosides

Peijiao Wang,[†] Jeremiah E. Miller,[‡] Lawrence M. Henling,[§] Charlotte L. Stern,[†] Natia L. Frank,[||] Amanda L. Eckermann,[†] and Thomas J. Meade*[,†,⊥,#]

Departments of Chemistry, Biochemistry and Molecular and Cell Biology, Neurobiology and Physiology and Radiology, Northwestern University, 2145 Sheridan Road, Evanston, Illinois 60208, University of Washington, School of Law, William H. Gates Hall, Box 353020 Seattle, Washington 98195, Beckman Institute, California Institute of Technology, Pasadena, California 91125, and Department of Chemistry, P.O. Box 3065, STN CSC, University of Victoria, Victoria, BC, V8W 3V6, Canada

Received June 25, 2007

We report the synthesis and characterization of new ruthenium and rhenium nucleosides [Ru(tolyl-acac)$_2$(IMPy)-T] (tolyl-acac = di(p-methylbenzonatemethane), IMPy = 2′-iminomethylpyridine, T = thymidine) (**5**) and [Re(CO)$_3$-(IMPy)-T]Cl (**9**), respectively. Structural analysis of **9** shows that the incorporation of this metal complex causes minimal perturbation to the sugar backbone and the nucleobase. Eletrochemical (**5**, $E_{1/2}$ = 0.265 V vs NHE; **9**, $E_{1/2}$ = 1.67 V vs NHE), absorption (**5**, λ_{max} = 600, 486 nm; **9**, λ_{max} = 388 nm), and emission (**9**, λ_{max} = 770 nm, π = 17 ns) data indicate that **5** and **9** are suitable probes for DNA-mediated ground-state electron-transfer studies. The separation and characterization of diastereoisomers of **5** and bipyridyl-based ruthenium nucleoside [Ru(bpy)$_2$-(IMPy)-T]$^{2+}$ (**7**) are reported.

Introduction

Redox- and photoactive transition-metal complexes that function as spectroscopic probes for photophysical studies in nucleic acids remain an active research area.[1−3] These complexes have been used to study long-range electron transfer (ET) and energy transfer in DNA,[1,2] DNA hybridization, and the development of biosensors.[3] For example, a commercially available biosensor for the electronic detection of the cystic fibrosis gene in potential carriers was FDA approved in January of 2006 (Osmetech, Pasadena, CA).

Methodologies for the incorporation of metal centers into oligonucleotides as probes include covalent attachment to, or intercalation in oligonucleotides where insertion sites are at the termini or within the DNA sequence.[1,4−10] Metal complexes have been covalently introduced into DNA using

* To whom correspondence should be addressed. E-mail: tmeade@northwestern.edu.

[†] Department of Chemistry, Northwestern University.

[‡] School of Law, University of Washington.

[§] Beckman Institute, California Institute of Technology.

[||] Department of Chemistry, University of Victoria.

[⊥] Department of Biochemistry and Molecular and Cell Biology, Northwestern University.

[#] Department of Neurobiology and Physiology and Radiology, Northwestern University.

(1) (a) Meade, T. J.; Kayyem, J. F. *Angew. Chem., Int. Ed. Engl.* **1995**, *34*, 352−354. (b) Kelley, S. O.; Barton, J. K. *Science* **1999**, *283*, 375−381. (c) Hurley, D. J.; Tor, Y. *J. Am. Chem. Soc.* **1998**, *120*, 2194−2195. Hurley, D. J.; Tor, Y. *J. Am. Chem. Soc.* **2002**, *124*, 13231−13241. (d) Weatherly, S. C.; Yang, I. V.; Thorp, H. H. *J. Am. Chem. Soc.* **2001**, *123*, 1236−1237. (e) Lewis, F. D.; Letsinger, R. L.; Wasielewski, M. R. *Acc. Chem. Res.* **2001**, *34(2)*, 159−170. Lewis, D. F.; Wasielewski, M. R. *Top. Curr. Chem.* **2004**, *236*, 45−65.

(2) (a) Brun, A. M.; Harriman, A. *J. Am. Chem. Soc.* **1992**, *114*, 3656−3660. Harriman, A. *Angew. Chem., Int. Ed.* **1999**, *38*, 945−949. (b) Olson, E. J. C.; Hu, D.; Hoermann, A.; Barbara, P. F. *J. Phys. Chem. B* **1997**, *101*, 299−303. (c) Giese, B. *Annu. Rev. Biochem.* **2002**, *71*, 51−70. (d) O'Neill, M. A.; Barton, J. K. *Top. Curr. Chem.* **2004**, *236*, 67−115.

(3) (a) Yu, C. J.; Wan, Y.; Yowanto, H.; Li, J.; Tao, C.; James, M. D.; Tan, C. L.; Blackburn, G. F.; Meade, T. J. *J. Am. Chem. Soc.* **2001**, *123*, 11155−11161. (b) Armistead, P. M.; Thorp, H. H. *Anal. Chem.* **2000**, *72*, 3764−3770. (c) Knemeyer, J. P.; Marme, N.; Sauer, M. *Anal. Chem.* **2000**, *72*, 3717−3724. (d) Wang, J. *Anal. Chim. Acta* **2002**, *469*, 63−71. (e) Odenthal, K. J.; Gooding, J. J. *Analyst* **2007**, *132*, 603−610.

(4) (a) Krider, E. S.; Meade, T. J. *J. Bio. Inorg. Chem.* **1998**, *3*, 222−225. (b) Rack, J. J.; Krider, E. S.; Meade, T. J. *J. Am. Chem. Soc.* **2000**, *122*, 6287−6288. (c) Krider, E. S.; Rack, J. J.; Frank, N. L.; Meade, T. J. *Inorg. Chem.* **2001**, *40*, 4002−4009.

(5) Frank, N. L.; Meade, T. J. *Inorg. Chem.* **2003**, *42*, 1039−1044.

(6) (a) Khan, S. I.; Grinstaff, M. W. *J. Am. Chem. Soc.* **1999**, *121*, 4704−4705. (b) Hu, X.; Smith, G. D.; Sykora, M.; Lee, S. J.; Grinstaff, M. W. *Inorg. Chem.* **2000**, *39*, 2500−2504.

(7) Manchanda, R.; Dunham, S. U.; Lippard, S. J. *J. Am. Chem. Soc.* **1996**, *118*, 5144−5145.

(8) Schliepe, J.; Berghoff, U.; Lippert, B.; Cech, D. *Angew. Chem., Int. Ed. Engl.* **1996**, *35*, 646−648.

(9) Elmroth, S. K. C.; Lippard, S. J. *J. Am. Chem. Soc.* **1994**, *116*, 3633−3634.

(10) Holmberg, R. C.; Tierney, M. T.; Ropp, P. A.; Berg, E. E.; Grinstaff, M. W.; Thorp, H. H. *Inorg. Chem.* **2003**, *42*, 6379−6387.

10.1021/ic701250r CCC: $37.00
Published on Web 10/19/2007

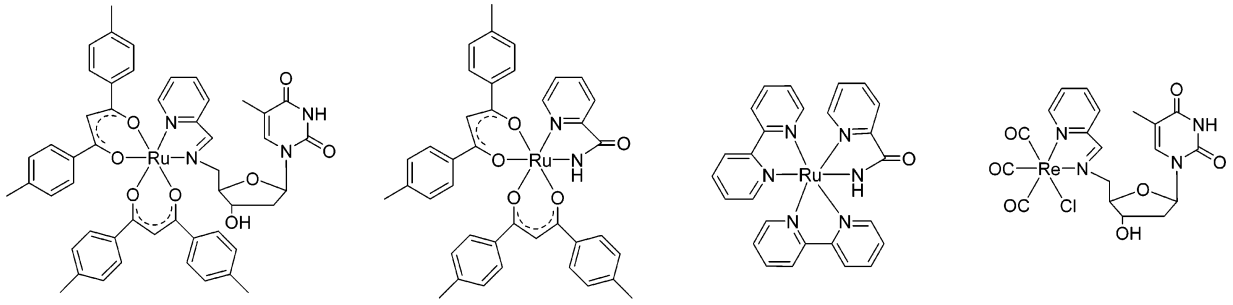

5 6 8 9

Figure 1. Structures of [Ru(tolyl-acac)$_2$(IMPy)-T] **5**, [Ru(tol-acac)$_2$(pyridine-2-carboxamide)] **6**, [Ru(bpy)$_2$(pyridine-2-carboxamide)]$^{2+}$ **8**, and [Re(CO)$_3$-(IMPy)-T]Cl **9**.

metalated phosphate or phosphoramidite monomers, where the metal complex (platinum(II), ruthenium(II), or osmium-(II)) is attached to the nucleoside base.[1(b),6−10] Additional examples include non-nucleosidic monomers, where the metal complex is tethered to the terminal phosphate group of the oligonucleotide.[11−14]

To use metal complexes for ET in DNA studies, our strategy focuses on the modification of DNA that fulfills the following requirements: (1) the distance and sequence between the terminal probes can be varied, (2) the modification should produce minimum structural perturbation to the nucleic base moiety and ribose ring, (3) a range of complexes with spectroscopically distinguishable characteristics and tunable redox potentials, and (4) the complex should be stable to automated DNA solid-phase synthesis with high yields.

We have reported site-selective incorporation of high- and low-potential electron donor and acceptor metal complexes in different positions of the DNA ribose backbone via solid-phase synthesis.[4,5] This approach offers rapid and efficient metal incorporation over biomolecular metalation techniques. The chemically stable bis(2,2′-bipyridine) ruthenium(II) complex has been tethered to DNA via the 5′ position of the ribose moiety.[4,5] A ruthenium(II) donor complex has not been successfully incorporated into oligonucleotides as a result of its instability during automated DNA synthesis.[4]

Here, we report the synthesis and characterization of new low- and high-potential donor and acceptor metal nucleosides.[15] Our approach involves the synthesis of ruthenium-(II) and rhenium(I) complexes that can be selectively attached to the 5′ position of the DNA backbone using standard automated phosphoramidite chemistry. We report the first structural characterization of a high-potential acceptor rhenium nucleoside (Figure 1). Spectroscopic and electrochemical characterization indicates that these metal complexes will not lead to guanine oxidation. We report the separation and characterization of diastereomers of a bis-(2,2′-bipyridine) ruthenium(II) acceptor and a bis(tolyl-acetylacetonate) ruthenium(II) donor.

Experimental Section

Materials and Methods. All of the reagents were purchased and used as received from Aldrich except for ruthenium(III) trichloride hydrate and *cis*-dichloro-bis(2,2′-bipyridine) ruthenium-(II), which were obtained from Strem. The ligand 1-(4-hydroxy-5-[(pyridin-2-ylmethylene)-amino]-methyl-tetrahydro-furan-2-yl)-5-methyl-1*H*-pyrimidine-2,4-dione (**4**) was prepared following literature procedures by refluxing 5′-amino-5′-deoxy-thymidine and 2-pyridinecarboxaldehyde in anhydrous ethanol with a yield of 82%.[16,17] Anhydrous solvents, where indicated, were obtained from Aldrich in Sure-Seal bottles. Water was purified using a Millipore Milli-Q Synthesis purifier. NMR spectra were recorded on either a Varian Mercury 400 MHz or a Varian Inova 500 MHz instrument. Peaks were referenced to an internal $Si(CH_3)_4$ standard. Electrospray mass spectra were obtained via direct infusion of a methanolic solution of the compound of interest on a Varian 1200L single quadrupole mass spectrometer. Elemental analyses were performed by Desert Analytics (Tucson, AZ). UV−vis spectroscopy was performed on a HP 8452A diode array spectrometer. Infrared spectra were measured in methylene chloride on a Biorad FTS-60 FT-IR spectrometer. Electrochemical experiments were performed on a Model 660A CH Instruments electrochemical analyzer. Cyclic voltammograms were measured at a scan rate of either 50 mV/s or 100 mV/s on 10^{-3} M CH_3CN solutions using 0.1 M Bu_4NPF_6 as a supporting electrolyte. A platinum wire counter electrode, a glassy carbon working electrode, and a Ag/AgCl reference electrode were used. Circular dichroism measurements were performed on a Jasco Model J-715 spectrometer with a 150 W air-cooled Xenon lamp as a light source.

Synthesis of 1,3-Di-(4-tolyl)-propane-1,3-dione (1). 1 was prepared by a modification of the literature procedure.[18] A solution of 4-methyl-benzoyl acid methyl ester (24.75 g, 165 mmol) and tolyl acetone (20.82 g, 150 mmol) in 10 mL dry THF, and 10 mL dry DMSO was added dropwise into a suspension of NaH (4 g, 166 mmol) in 45 mL dry THF and 35 mL dry DMSO under an argon atmosphere at 3∼5 °C with vigorous stirring. The addition process was finished within 50 min. After the addition, the reaction temperature was raised to 20 °C within 30 min. The reaction was stopped after stirring further at 30 °C for 50 min. Solvents were then removed in vacuo to give a brown solid. This solid was washed

(11) Hall, J.; Husken, D.; Pieles, U.; Moser, H. E.; Haner, R. *Chem. Biol.* **1994**, *1*, 185−190.
(12) Magda, D.; Crofts, S.; Lin, A.; Miles, D.; Wright, M.; Sessler, J. L. *J. Am. Chem. Soc.* **1997**, *119*, 2293−2294.
(13) Meggers, E.; Kusch, D.; Giese, B. *Helv. Chim. Acta* **1997**, *80*, 640−652.
(14) Khan, S. I.; Beilstein, A. E.; Sykora, M.; Smith, G. D.; Hu, X.; Grinstaff, M. W. *Inorg. Chem.* **1999**, *38*, 3922−3925.
(15) Here, we define a complex having $E_{1/2}$ > 800 mV versus NHE as a high-potential complex and a complex having $E_{1/2}$ < 300 mV versus NHE as a low-potential complex.
(16) Yamamoto, I.; Sekine, M.; Hata, T. *J. Chem. Soc., Perkin Trans.* **1980**, *1*, 306−310.
(17) Horwitz, J. P.; Tomson, A. J.; Urbanski, J. A.; Chura, J. *J. Org. Chem.* **1962**, *27*, 3045−3048.
(18) Franek, W. *Monatshefte für Chemie* **1996**, *127*, 895−907.

Table 1. Crystal Data and Structure Refinement Details for **6**, **8**, and **9**

	6	**8**·BF_4·$2CH_2Cl_2$	**9**
empirical formula	$C_{41}H_{35}N_2O_5Ru$	$C_{28}H_{24}BCl_4F_4N_6ORu$	$C_{22}H_{23}ClN_4O_8Re$
fw	725.33	790.21	693.09
cryst syst	monoclinic	monoclinic	monoclinic
space group	*Cc*	*P*2(1)/*c*	*C*2
a (Å)	15.5562(16)	13.351(3)	18.9576(10)
b	16.9163(17)	24.925(5)	9.5095(5)
c (Å)	14.3802(14)	19.879(4)	12.4516(8)
α (deg)	90.00	90.00	90.00
β (deg)	110.859(2)	103.494(16)	100.4950(10)
γ (deg)	90.00	90.00	90.00
V (Å^3)	3536.2(6)	6433(2)	2561.7(2)
Z	4	8	4
ρ_{calcd} (mg/m^3)	1.383	1.632	1.797
μ (mm^{-1})	0.486	0.877	4.900
F (000)	1516	3160	1356
cryst size (mm^3)	0.290 × 0.260 × 0.200	0.446 × 0.276 × 0.072	0.290 × 0.240 × 0.150
reflns collected	16 162	58 971	26 077
reflns observed	8149, R(int) = 0.0192	15 642, R(int) = 0.1004	5908, R(int) = 0.0786
data/restraints/params	8149/2/465	15 642/0/613	5908/7/303
GOF on F^2	1.103	0.981	2.010
Final R indices [$I > 2\sigma(I)$]	0.0432, 0.1108	0.0743, 0.2099	0.0337, 0.0806
R indices (all data) R1[a], wR2[b]	0.0460, 0.1140	0.1237, 0.2251	0.0356, 0.0810
largest diff. peak/hole (e,Å^{-3})	1.706/−0.445	1.504/−1.845	2.336/−1.033

[a] $R1 = \sum| |F_o| - |F_c| |/\sum|F_o|$. [b] $wR2 = \{\sum[w(F_o^2 - F_c^2)^2]/\sum[w(F_o^2)^2]\}^{1/2}$.

Scheme 1[a]

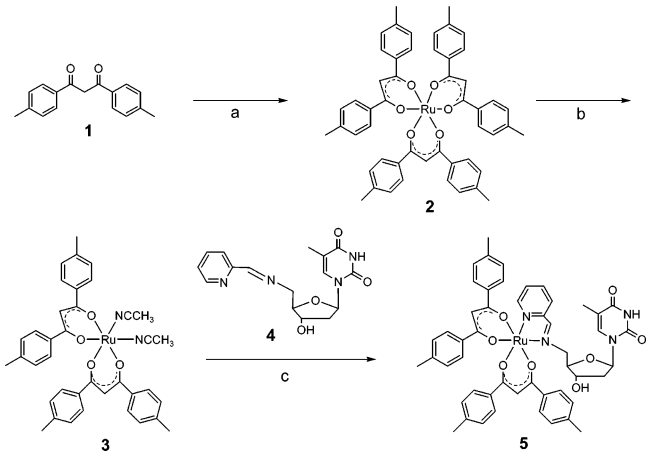

[a] Reagents: (a) $RuCl_3$·xH_2O, EtOH, H_2O, reflux 4h; $NaHCO_3$ reflux 3h, 24%; (b) Zn-Hg, CH_3CN, H_2O, 80%; (c) EtOH, reflux, 65%.

with 250 mL dry ether and dried in vacuo. The resulting light-brown solid was added to 400 mL ice−water in a beaker, and 20 mL concentrated (33%) hydrochloric acid was added right afterward with vigorous stirring. A tan solid formed and was filtered. The obtained solid was washed with 100 mL distilled water, filtered, and dried in vacuo. Yield : 26.50 g (80%). ^{1}H NMR (acetone-d_6, 400 MHz): δ 8.01(d, J = 8 Hz, 4H), 7.32 (d, J = 8.5 Hz, 4H), 7.16 (s, 1H); 2.81 (s, 2H); 2.38 (d, J = 9.6 Hz, 6H). ESI-MS Calcd $[M+H]^+$ 253.2, $[M+Na]^+$ 275.2, Found $[M+H]^+$253.3, $[M+Na]^+$ 275.

Synthesis of Tris-(di-p-methyl-benzoate Methane) Ruthenium(III) (2). The procedure was followed as previously reported.[19,20] A dark-red solution of $RuCl_3$·xH_2O (3.00 g, 14.4 mmol) was prepared using 300 mL ethanol/150 mL H_2O. The flask was equipped with a reflux condenser and an argon inlet and was heated to reflux for 4 h, resulting in a deep-blue/green solution ("ruthenium blue"). After refluxing, the solution was cooled to room temperature and ligand **1** (13 g, 60 mmol) was added to the solution under argon. The reaction was then brought to reflux again for 45 min, resulting in a deep-red solution. Sodium carbonate (7.2 g, 87.0 mmol) was added in two portions over this time. After the addition, the solution mixture refluxed until no gas evolution was observed (around 3 h). The reaction solution was then cooled to room temperature. The solvent was removed until about 150 mL remained. Vacuum filtration of this remaining reaction mixture left a black sticky solid and a deep-red supernatant. The black solid was washed with 10 × 20 mL acetone, and the deep-red supernatants were combined (TLC showed these contained the product). The solvent was removed in vacuo to give a red solid. The solid was purified by column chromatography on silica with 4:1 (v/v) dichloromethane/hexane to give red crystals. Yield: 2.8 g (24%). ^{1}H NMR (C_6D_6, 400 MHz): δ6.20 (s, 24H), 0.41 (s, 18H), −32.8 (s, 3H). ESI-

(19) Endo, A.; Shimzu, K.; Sato, G. P.; Mukaida, M. *Chem. Lett.* **1984**, 437−440.
(20) Miller, J. E. Ph.D. Thesis, California Institute of Technology, Pasadena, CA, 2003.

Table 2. Half-Wave Potentials and MLCT Absorption of $Ru(acac)_2(IMPy\text{-}T)$ and **5**, **7**, **9**

	$E_{1/2}$ (V vs NHE)[a]	MLCT λ_{max}, nm (ϵ $M^{-1}cm^{-1}$)[c]
$Ru(acac)_2(IMPy\text{-}T)$	0.236[b]	402 (4600)[d] 586 (4600)[d]
$Ru(tol\text{-}acac)_2(IMPy\text{-}T)$ (**5**)	0.265	486 (4400) 600 (5200)
$[Ru(bpy)_2(IMPy\text{-}T)].2PF_6$ (**7**)	1.357	464 (7500)
$[Re(CO)_3(IMPy\text{-}T)]Cl$ (**9**)	1.67	388 (3400)[e]

0.1 M $^tBu_4NPF/CH_3CN$ (0.1 M) at a scan rate of 0.05 V/s.[b] 0.1 M $^tBu_4NPF_6$/EtOH at a scan rate of 0.1 V/s (ref 5). [c] In MeOH. [d] In EtOH (ref 5). [e] In 50 mM NaH_2PO_4/Na_2HPO_4, 75 mM NaCl buffer, pH 6.70.

MS Calcd for $C_{51}H_{45}O_6Ru$ $[M]^+$ 855.2, Found $[M+H]^+$ 856.2, $[M+Na]^+$ 878.2.

Synthesis of Bis-(di-p-methyl-benzoate methane) Ruthenium-(II) *cis*-Bis(acetonitrile) (3). 2 (200 mg, 0.25 mmol) was suspended in a mixture of 42.5 mL CH_3CN and 7.5 mL H_2O. The suspension was degassed by argon sparge for 20 min. Approximately 10 g Zn−Hg amalgam was added to this suspension, and the reaction was brought to reflux (around 95 °C) under argon. The solution showed color changes from brown to blue, to green, to dark green, to red over 40 min. The red solution was then held at reflux for 5.5 h. The reaction mixture was cooled to room temperature and filtered to give a clear red solution. The solvent was removed in vacuo to give a red powder. Yield: 130 mg (78%), stored under argon. ^1H NMR (acetone-d_6, 500 MHz): δ 7.94 (d, J = 7.7 Hz, 4H), 7.77 (d, J = 7.8 Hz, 4H), 7.23 (d, J = 7.7 Hz, 4H), 7.07 (d, J = 7.7 Hz, 4H), 6.69 (s, 2H), 2.69 (s, 6H), 2.34 (s, 6H), 2.24 (s, 6H). ESI-MS Calcd for $C_{38}H_{36}N_2O_4Ru$ $[M]^+$ 686.2, Found $[M]^+$ 686.2.

Syntheses of Bis-di(p-methylbenzonatemethane)ruthenium-(II)(1-(4-Hydroxy-5-[(pyridin-2-ylmethylene)-amino]-methyl-tetrahydro-furan-2-yl)-5-methyl-1*H*-pyrimidine-2,4-dione) (5) and Bis-di(p-methylbenzonatemethane)ruthenium(II)[(pyridin-2-one)-amino] (6). 4 (137 mg, 0.41mmol) was dissolved in 50 mL anhydrous ethanol to give a colorless solution. The solution was degassed for 45 min under argon sparge. **3** (280 mg, 0.41 mmol) was added under argon to give a dark-red solution. The reaction was brought to reflux for 1.5 h, resulting in a dark-green solution. The solution was cooled to room temperature, and ethanol was removed in vacuo to give a dark-green solid. This material was purified by column chromatography on silica gel using 4:1 (v/v) CH_2Cl_2/THF to give the diastereomeric mixture as a dark-green powder **5**, Yield: 243 mg (65%) and dark-red crystals **6**, Yield: 98 mg (31%).

^1H NMR (CD_3CN, 500 MHz) of **5:** δ 8.95 (s, 1H), 8.87 (s, 0.5H), 8.82 (s, 0.5H), 8.66 (s, 2H), 7.90−7.94 (t, J = 8.4, 7.9 Hz, 6H), 7.70−7.82 (d, J = 7.9 Hz, 2H), 7.68 (s, 2H), 7.5−7.6 (m, 6H), 7.06−7.22 (m, 16H), 6.95 (s, 1H), 6.19−6.26 (m, 1H), 5.04−5.07 (m, 1H), 4.08−4.63 (m, 5H), 3.75 (d, J = 4.02 Hz, 2H), 2.25−2.32 (m, 23H), 1.79 (s, 3H), 0.94 (s, 3H). ESI-MS calcd for $[M]^+$ 934.2, found $[M]^+$ 934.2. UV−vis (MeOH): λ_{max} nm (ϵ) 266 (20,-100), 330 (23,400), 486 (4,400), 600 (5,200). $E_{1/2}$ (CH_3CN) = 0.265 V versus NHE.

^1H NMR (CD_3CN, 500 MHz) of **6:** δ 8.63−8.96 (m, 4H), 7.78−7.93 (m, 8H), 7.23−7.35 (m, 8H), 6.96 (s, 1H), 2.35−2.38 (m, 12H). ESI-MS of **6:** calcd for $C_{40}H_{35}N_2O_5Ru$: $[M]^+$ 725, found $[M]^+$ 725.3.

Purification of Bis(2,2′-bipyridine)ruthenium(II)(1-(4-Hydroxy-5-[(pyridin-2-ylmethylene)-amino]-methyl-tetrahydro-furan-2-yl)-5-methyl-1*H*-pyrimidine-2,4-dione) (7) and Bis(2,2′-bipyridine)ruthenium(II)[(pyridin-2-one)-amino] (8). The literature procedure for **7** was followed.[5] This mixture was further purified from the unreacted *cis*-dichloro-bis(2,2′-bipyridine)ruthenium(II) by two columns. The first silica gel column used 80%:16%:4% (v/v/v) acetonitrile/water/saturated KNO_3 solution as the eluent (R_f = 0.2). A second column used the SP-Sephadex C-25 cation exchange column (40 × 200 mm) eluting with 0.05M NaCl.

7 appeared as the second red band after 14 h elution (R_f = 0.15). The compound was precipitated by the addition of saturated KPF_6, and the solid was collected by vacuum filtration and washed with water (2 × 10 mL). A red solid was obtained after drying in vacuo. Yield: 334 mg (55%). ^1H NMR (CD_3CN, 500 MHz): δ 9.29 (s, 1H), 9.21 (s, 1H), 9.12 (s, 1H), 9.07 (s, 1H), 8.46−8.65 (m, 10H), 8.4(d, J = 4.8 Hz, 1H), 8.30−8.35 (m, 2H), 8.02−8.27 (m, 11H), 7.77−7.85 (m, 4H), 7.37−7.69 (m, 15H), 7.14 (s, 1H), 7.11(s, 1H), 6.07 (t, J = 6.8, 7.6 Hz, 1H), 5.8 (t, J = 6.8, 6.5 Hz, 1H), 4.04 (d, J = 5.8 Hz, 4H), 3.83−3.89 (m, 2H), 3.66 (m, 1H), 3.43 (d, J = 4.6 Hz, 1H), 3.35 (d, J = 4.9 Hz, 1H), 3.15 (d, J = 5.5 Hz, 1H), 2.26−2.33 (m, 7H), 2.04−2.15 (m, 3H). ESI-MS Calcd for $[MPF_6]^+$ 889.14, Found $[MPF_6]^+$ 889.24. UV−vis (MeOH): λ_{max} nm (ϵ) 210 (42,000), 246 (25,000), 288 (49,000), 464 (7,500). Elemental analysis (EA): Calcd for M+2PF_6: $C_{36}H_{34}F_{12}N_8O_4P_2Ru$: C, 41.83; H, 3.32; N, 10.84. Found: C, 41.89; H, 3.56; N, 11.10. $E_{1/2}$ (CH_3CN) = 1.36 V versus NHE.

8 appeared as a third red band after 16 h elution (R_f = 0.1). The eluted fraction was precipitated with saturated KPF_6. The solid was collected by vacuum filtration and washed with water (2 × 10 mL). A red solid was obtained after it was dried in vacuo. Yield: 173 mg (48%). ^1H NMR (CD_3CN, 500 MHz): δ 9.64 (s, 0.5H), 8.81 (d, J = 5.3 Hz, 1H), 8.39−8.51 (m, 4H), 8.04 (t, J = 6.2, 7.7 Hz, 3H), 7.94 (d, J = 5.1 Hz, 1H), 7.85−7.91 (m, 4H), 7.64 (t, J = 7.3, 5.3 Hz, 2H), 7.49 (t, J = 4.2, 7.3 Hz, 2H), 7.33 (t, J = 6.4, 6.2 Hz, 1H), 7.21−7.26 (m, 3H). ESI-MS of **8**: Calcd for $C_{26}H_{21}F_6N_6OPRu$: $[MPF_6]^+$ 680.05, Found $[MPF_6]^+$ 680.3.

Synthesis of Rhenium (I) tricarbonyl chloride (1-(4-Hydroxy-5-[(pyridin-2-ylmethylene)-amino]-methyl]-tetrahydro-furan-2-yl)-5-methyl-1H-pyrimidine-2,4-dione) (9). $Re(CO)_5Cl$ (0.240 g, 0.66 mmol) and **4** (0.240 g, 0.73 mmol) were dissolved in 15 mL THF, to give a clear greenish solution with a white solid. This solution was degassed by argon sparge and equipped with a reflux condenser, under argon. The solution was heated to reflux in a water bath, and all of the material dissolved after 5 min. Reflux was continued for an additional 70 min, during which time the greenish solution turned deep-orange and cloudy. The orange suspension was filtered to give an orange solution and a greenish solid. The solid was washed with THF, and the washings were combined with the filtrate. The THF was removed in vacuo to give an orange solid. TLC on silica gel with a 90:10 CH_2Cl_2/MeOH eluent showed a deep yellow spot (R_f = 0.57) and four UV-active spots. The bulk solid was purified on silica gel with the same eluent to give **9**. Yield: 0.234 g (53%). ^1H NMR (CD_3CN, 300 MHz) δ 9.03 (m, 2H), 8.92 (m, 1H), 8.20 (m, 1H), 8.10 (m, 1H), 7.70 (m, 1H), 7.30 (brs, 1H), 6.23 (t, J = 7 Hz, 1H), 4.4 (m, 6H), 3.74 (d, J = 4 Hz, 2H), 2.40 (m, 2H), 2.30 (m, 2H), 1.83 (d, J = 1.5 Hz, 3H) ^{13}C NMR (CD_3CN, 125.7 MHz) δ 171.4 (s), 164.6 (s), 155.7 (s), 155.7 (s), 154.2 (s), 151.4 (s), 141.4 (s), 137.6 (s), 130.3(s), 111.8 (s), 86.5 (s), 84.6 (s), 72.5 (s), 66.9 (s), 39.0 (s), 12.4 (s). UV−vis ((H_2O) λ_{max} nm (ϵ)) 202 (26,000), 266 (17,600), 388 (3,400), 400 (3,100), 420 (2,100). IR: (CH_2Cl_2) ν 2025.6 cm^{-1}, 1925.4 cm^{-1}, 1905.0 cm^{-1}, 1712.5 cm^{-1}, 1693.3 cm^{-1}, 1602.6 cm^{-1}. ESI-MS Calcd $[M+H]^+$ 601.07, found $[M+H]^+$ 601.0 (rhenium isotope pattern apparent). $E_{1/2}$ (ox) (CH_3CN) = 1.67 V versus NHE, $E_{1/2}$ (red) (CH_3CN) = −0.81 V versus NHE.

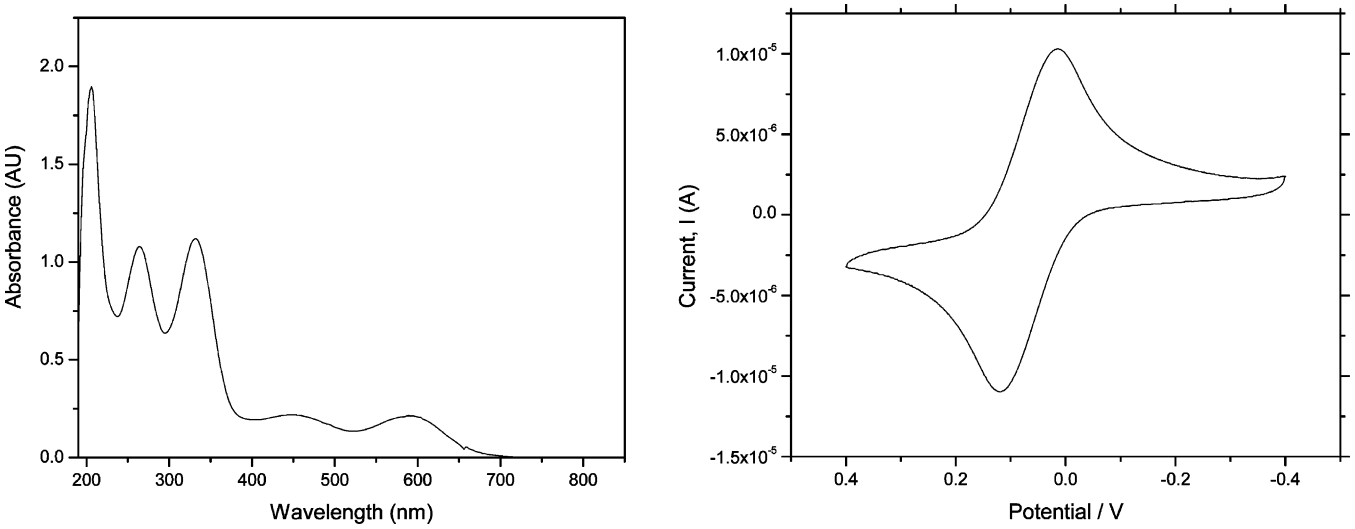

Figure 2. (a) UV-vis absorption spectrum of **5** in MeOH. (b) Room-temperature cyclic voltammogram of **5** in 0.1 M $^{t}Bu_4NPF_6/CH_3CN$ at a scan rate of 0.05 V/s, $E_{1/2}$ for **5** is 0.265 V versus NHE.

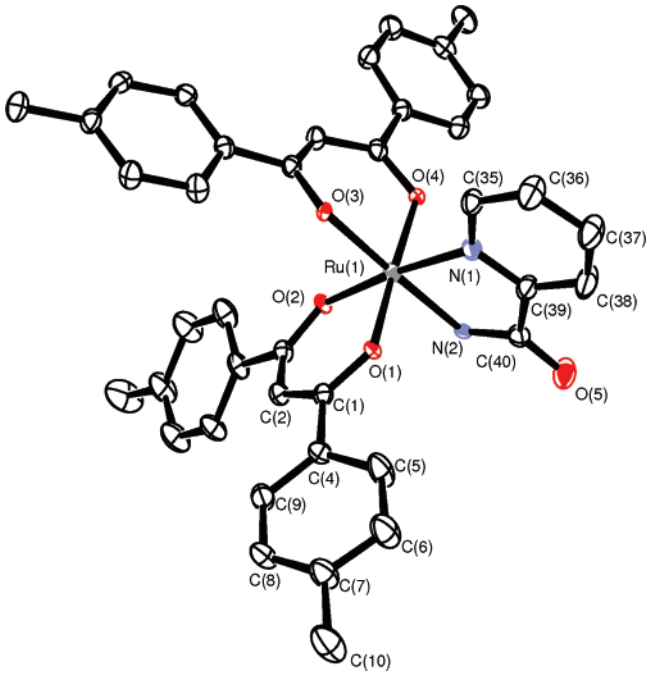

Figure 3. ORTEP view of [Ru(tol-acac)$_2$(pyridine-2-carboxamide)] **6** drawn with 30% probability thermal ellipsoids. Hydrogen atoms and solvent molecules are omitted for clarity. Selected bond lengths (Å) and bond angles (deg) are as follows. Ru−O(3) 1.986(4), Ru−O(1) 1.989(2), Ru−O(4) 1.994(2), Ru−O(2) 2.029(2), Ru−N(2) 2.021(4), Ru−N(1) 2.024(3), C(40)−O(5) 1.223(5), O(3)−Ru−O(4) 89.57(11), O(1)−Ru−O(2) 92.66(10), O(3)−Ru−O(1) 90.58(10), N(2)−Ru−N(1) 80.59(15), O(4)−Ru−N(1) 90.66(11), O(1)−Ru−N(1) 85.67(11), C(39)−N(1)−Ru 113.6(2), C(40)−N(2)−Ru 115.6(3), O(5)−C(40)−N(2) 124.6(4).

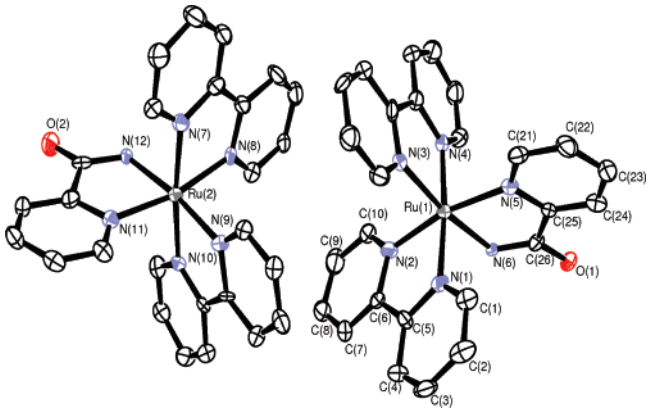

Figure 4. ORTEP view of [Ru(bpy)$_2$(pyridine-2-carboxamide)]$^{2+}$ **8** drawn with 30% probability thermal ellipsoids. Hydrogen atoms and solvent molecules are omitted for clarity. Selected bond lengths (Å) and bond angles (deg) are as follow. Ru(1)−N(1) 2.037(4), Ru(1)−N(2) 2.039(4), Ru(1)−N(4) 2.042(4), Ru(1)−N(3) 2.054(4), Ru(1)−N(5) 2.066(4), Ru(1)−N(6) 2.083(3), Ru(2)−N(9) 2.029(5), Ru(2)−N(11) 2.050(5), Ru(2)−N(10) 2.052(5), Ru(2)−N(8) 2.056(5), Ru(2)−N(7) 2.059(5), Ru(2)−N(12) 2.086-(4), O(1)−C(26) 1.232(6), O(2)−C(52) 1.217(7), N(1)−Ru(1)−N(2) 78.72-(17), N(1)−Ru(1)−N(3) 97.89(16), N(4)−Ru(1)−N(3) 79.63(16), N(3)−Ru(1)−N(5) 96.41(16), N(1)−Ru(1)−N(6) 89.60(15), N(5)−Ru(1)−N(6) 79.27(16), C(25)−N(5)−Ru(1) 113.2(3), C(26)−N(6)−Ru(1) 115.6(3), O(1)−C(26)−N(6) 124.7(5).

Diastereoisomer Separation. The separation of diastereoisomeric **5** (100 mg, 0.1mmol) was achieved using a 40 × 200 mm silica column and CH_2Cl_2/THF (4:1,v/v) as the eluents. Two dark-green bands separated (*f* 1, $R_f = 0.18$; *f* 2, $R_f = 0.3$). The solvents were removed for each diastereoisomer in vacuo. Further removal of trace impurities for each diastereoisomer was performed by a silica gel column with neat toluene as the eluent. The solvents were removed in vacuo and two dark-green powders of band 1 as **Λ5** and band 2 as **Δ5**[21] were obtained after drying in vacuo. Yields: **Λ5** 62 mg (62%), **Δ5** 34 mg (34%). ^{1}H NMR (CD_3CN, 500 MHz) of **Λ5**: δ 8.8 (s, 2H), 8.6 (s, 2H), 7.25−7.95 (m, 8H), 7.05−7.2 (m, 8H), 6.95 (s, 1H), 6.5 (m, 1H), 6.2 (s, 1H), 5.05 (s, 1H), 4.05−4.6 (m, 5H), 3.75 (s, 2H), 2.2−2.4 (m, 12H), 0.7 (s, 3H). ^{1}H NMR (CD_3CN, 500 MHz) of **Δ5:** δ 8.82 (s, 2H), 8.6 (s, 2H), 7.75−8 (m, 2H), 7.25−7.74 (m, 6H), 7.05−7.23 (m, 8H), 6.93 (s, 1H), 6.4 (s, 1H), 6.2 (s, 1H), 5.03 (s, 1H), 4.02−4.57 (m, 5H), 3.72 (s, 2H), 2.18−2.45 (m, 12H), 0.6 (s, 3H).

The diastereoisomeric separation of purified **7** was accomplished by cation exchange chromatography. As isolated by the above procedure, **7** (100 mg) was converted into the chloride salt by metathesis with NH_4Cl in acetone. The solid was collected by filtration through celite and washed through with water (50 mL). The volume of water was reduced to approximately 5 mL in vacuo, and the resulting dark-red solution was introduced onto a SP Sephadex C25 column (dimensions 2 × 100 cm). A solution of 0.15 M sodium (-)-*O*,*O*′-dibenzoyl-L-tartrate (prepared by the

(21) Assigned according to the CD spectra of bands 1 and 2 of **5** and bands 1 and 2 of **7**, respectively.

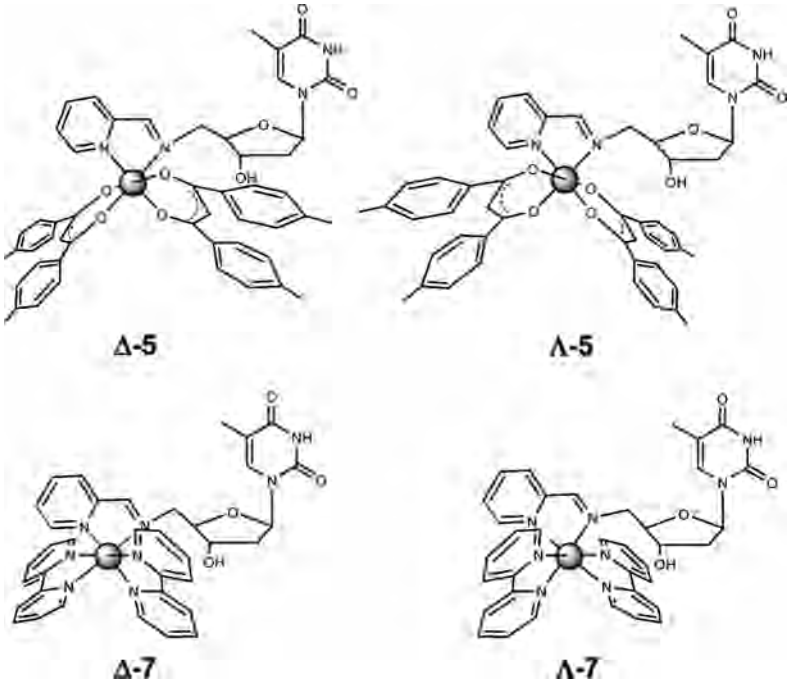

Figure 5. Structures of Δ/Λ [Ru(tolyl-acac)$_2$(IMPy-T] **5** and Δ/Λ [Ru(bpy)$_2$(IMPy-T]$^{2+}$ **7**.

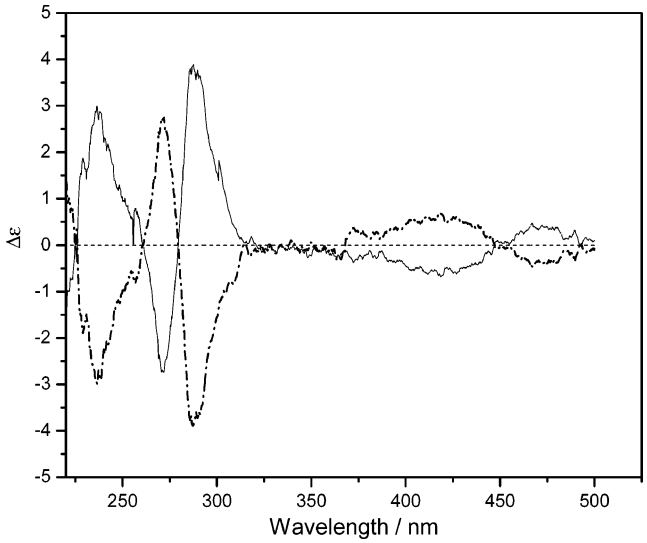

Figure 6. CD spectra of Λ-**7** (solid line) and Δ-**7** (dashed line) in acetonitrile.

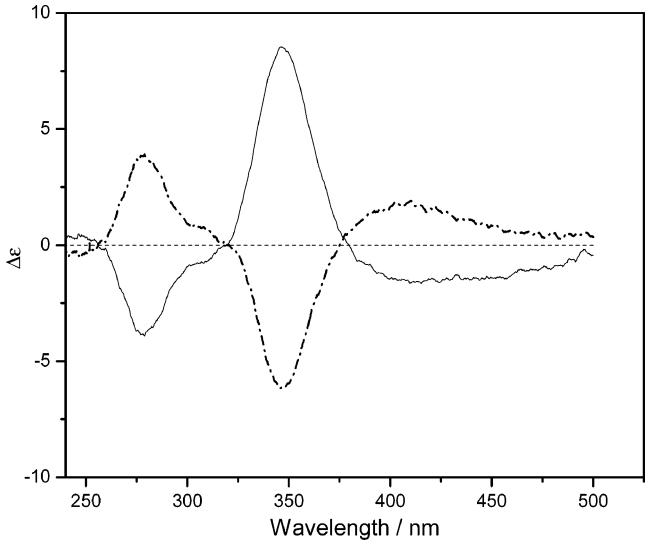

Figure 7. CD spectra of Λ-**5** (solid line) and Δ-**5** (dashed line) in acetonitrile.

neutralization of the acid with sodium hydroxide) was used as the eluent. An eluent flow of 1.5 mL/min was regulated by the use of a peristaltic pump. Two red bands separated after an effective column length[22] of 1−1.5 m. After separation, each band was subjected to the following procedure. The solution was reduced in volume to 50 mL and converted into the hexafluorophosphate salt by the addition of potassium hexafluorophosphate. The precipitates were collected by vacuum filtration and washed with water (2 × 20 mL). The extra tartrate salts were further removed by a short silica column (40 × 50 mm) washing with 30 mL water, 30 mL acetonitrile, and 50 mL water. The complex was eluted from the column using 30 mL saturated ammonium hexafluorophosphate in acetonitrile. To this solution was added an equal amount of water and the total volume reduced to 30∼40 mL in vacuo. The hexafluorophosphate salt of the diastereoisomer precipitated and was filtered and washed with water and anhydrous diethyl ether. Two red solids of band 1 as Λ**7** and band 2 as Δ**7**[21] were obtained after drying in vacuo. Yields: Λ**7** 33 mg (33%), Δ**7** 15 mg (15%). ^{1}H NMR (CD_3CN, 500 MHz) of Λ**7:** δ 8.88−8.97 (m, 2H), 7.91−8.49 (m, 8H), 7.24−7.89 (m, 8H), 6.97 (d, J = 13.54 Hz, 1H), 5.91 (d, J = 6 Hz, 1H), 5.66 (d, J = 6.8 Hz, 1H), 3.89 (s, 2H), 3.52−3.74 (m, 2H), 3.0−3.26 (m, 6H), 2.04−2.19 (m, 3H). ^{1}H NMR (CD_3CN, 500 MHz) of Δ**7:** δ 8.92−9.0 (m, 2H), 7.9−8.45 (m, 8H), 7.26−7.9 (m, 8H), 6.97 (d, J = 13.7 Hz, 1H), 5.92 (s, 1H), 5.65 (s, 1H), 4.15 (s, 2H), 3.88 (s, 2H), 3.53−3.73 (m, 4H), 3.25 (s, 2H), 2.03−2.2 (m, 3H).

X-ray Crystallography. Diffraction quality crystals of **6** grew as red blocks by slow diffusion of pentane into an anhydrous methanol solution within a week. **8**·PF_6 was converted to the BF_4 salt by metathesis with $NaBF_4$. Crystals of **8**·BF_4 suitable for X-ray diffraction grew as red tabulates from slow diffusion of pentane

(22) Fletcher, N. C.; Junk, P. C.; Reitsma, D. A.; Keene, F. R. *J. Chem. Soc., Dalton Trans.* **1998**, 133−138.

Scheme 2

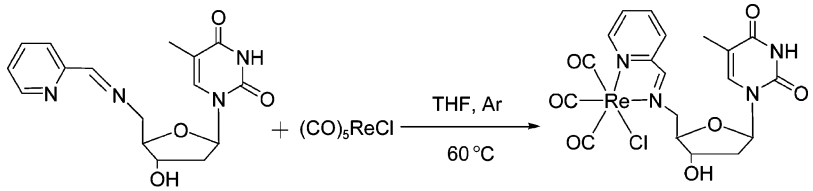

4 **9**

into a dichloromethane solution. Crystals of **9** grew as orange blocks from slow vapor diffusion of heptane into an acetone solution.

Crystallographic data were collected on a Bruker SMART 1000 X-ray diffractometer with a CCD detector using graphite-monochromated Mo Kα radiation ($\lambda = 0.71073$ Å). Data sets for **6** and **8** were obtained at 153(2) K. The data set for **9** was collected at 98(2) K. For **6**, the θ range for data collection was 1.85−28.87°, and data were collected in 0.3° oscillations with 5 s exposures. For **8**, the θ range for data collection was 1.33−28.97°, and data were collected in 0.3° oscillations with 20 s exposures. For **9**, the θ range for data collection was 2.19−28.23°. The crystal-to-detector distance was 50.00 mm, with the detector at the 28° swing position for all of the crystals. The linear absorption coefficient, μ, for Mo Kα radiation is 0.877 mm^{-1}. An analytical absorption correction was applied. Data were processed using *SAINT-NT* from Bruker and were corrected for Lorentz and polarization effects. The structures were solved by direct methods,[23] expanded using Fourier techniques, and refined by full matrix least-squares on F^2.[24] The non-hydrogen atoms were refined anisotropically. Hydrogen atoms were included but not refined.

Crystal data and refinement details of **6**, **8**, and **9** are summarized in Table 1.

Circular Dichroism. CD spectra were collected at 25 °C in a 1 cm path length cell at a bandwidth of 1 nm, a data pitch of 0.2 nm, and a response time of 2 s. The concentration of **5** and **7** were 2×10^{-6} M in spectral-grade acetonitrile. The CD spectra of diastereoisomers of **5** and **7** were obtained after substracting the absorption change ($\Delta\epsilon$) from the thymidine in acetonitrile. The concentrations of the thymidine solutions were calibrated by UV-vis to the same concentration of **5** and **7**.

Results and Discussion

Synthesis and Characterizations of Low-Potential Ruthenium Nucleoside. Previous work in our laboratory studied the high-potential metal complex $[Ru(bpy)_2(IM\ Py)\text{-}T]^{2+}$ (**7**) (IMPy = 2′-iminomethylpyridine, T = thymidine) and a low-potential complex $[Ru(acac)_2(IMPy)\text{-}T]$ to measure ground-state ET in DNA.[4,5] Modification of the 5′ position of thymidine by covalent attachment of IMPy allows access to both metal complexes and does not complicate the phosphoramidition at the 3′ position, which is necessary for the incorporation of metal nucleosides into DNA.[5] The high-potential metal nucleoside $[Ru(bpy)_2(IMPy)\text{-}T]^{2+}$ has been successfully incorporated into oligonucleotides by the 3′ position phosphoramidation strategy.[4] Incorporation of the low-potential nucleoside $[Ru(acac)_2(IMPy)\text{-}T]$, however, was unsuccessful as a result of its instability to both the mildly acidic and strongly basic solutions encountered in automated DNA synthesis.[4] Therefore, the synthesis of a stable low-potential ruthenium complex for incorporation into oligonucleotides was a target of our investigation.

We chose the tolyl group to replace the methyl groups of the acetylacetonate ligand based on the work of Haga et al. that showed an increase in the oxidation potential of bis-(dibenzonate methane) ruthenium(II) 2,2′-bipyridine over bis-(acetylacetonate) ruthenium(II) 2,2′-bipyridine.[20,25] Scheme 1 shows the synthetic approach to low-potential **5** (Figure 1). **1** was prepared from the reaction of 4-methyl-benzoyl acid-methyl ester and tolyl acetone with NaH in 80% yield.[18] Tris-(dibenzonate methane) ruthenium (III) **2** was synthesized from ruthenium (III) trichloride.[19] Reduction with Zn−Hg amalgam in acetonitrile and water produced bis-(dibenzonate methane) ruthenium(II) *cis*-bis(acetonitrile) **3** in high yield. Addition of **4**[16,17] in refluxing ethanol gave the final diastereomeric mixture of **5** in 65% yield and one side product **6** (Figure 1) in 31% yield.

A summary of metal-to-ligand charge transfer (MLCT) absorption and half-wave potentials of **5**, **7**, **9** (Figure 1), and related complexes are listed in Table 2. Spectroscopic characterization of **5** is shown in part a of Figure 2. A MLCT transition appears at 486 nm ($\epsilon = 4400$ L $mol^{-1}cm^{-1}$) in methanol and is assigned to ruthenium(II)−(tolyl-acac) $d(\pi)-\pi^*$ transition. The peak at 600 nm ($\epsilon = 5200$ L $mol^{-1}cm^{-1}$) was assigned to the ruthenium(II) (IMPy) $d(\pi)-\pi^*$ transition.[5] These values demonstrate a red shift of the MLCT bonds of **5** compared to $[Ru(acac)_2(IMPy\text{-}T)]$, which has MLCT transitions at 402 and 586 nm.[26] This shift results from a lower-energy π^* acceptor orbital in a tolylacac ligand compared to that of acetylacetonate ligand.

The redox potential of **5** was determined by cyclic voltammetry to be 0.265 V versus NHE (part b of Figure 2), which is ∼30 mV more positive than that of $[Ru(acac)_2\text{-}(IMPy\text{-}T)]$ (0.236 V vs NHE, Table 2). This small potential shift of **5** is a result of less electron density at the metal due to delocalization of the electrons over an extended π^* framework in **5**.[27] This is consistent with the MLCT band shift of **5** and should therefore be stable to automated DNA synthesis conditions. Given the oxidation potential of guanine

(23) Sheldrick, G. M. *SHELXS-97, Program for Crystal Structure Determination*; University of Göttingen: Göttingen, Germany, 1997.
(24) Sheldrick, G. M. *SHELXL-97, Program for the Refinement of Crystal Structures*; University of Göttingen: Göttingen, Germany, 1997.
(25) Haga, M. A.; Takeko, M. I.; Shimizu, K.; Sato, G. P. *J. Chem. Soc., Dalton Trans.* **1989**, 371−373.
(26) Hasegawa, T.; Lau, T. C.; Taube, H.; Schaefer, W. P. *Inorg. Chem.* **1991**, *30*, 2921−2928.
(27) Anderson, P. A.; Keene, F. R.; Meyer, T. J.; Moss, J. A.; Strouse, G. F.; Treadway, J. A. *J. Chem. Soc., Dalton. Trans.* **2002**, *20*, 3820−3831.

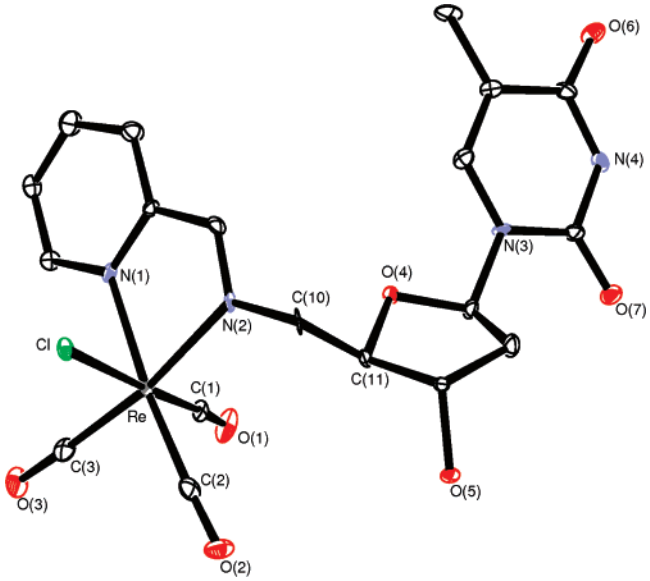

Figure 8. ORTEP view of $[Re(CO)_3(IMPy\text{-}T]Cl$ **9** drawn with 30% probability thermal ellipsoids. Hydrogen atoms and solvent molecules are omitted for clarity. Selected bond distances (Å) and angles (deg) are as follow. Re−C(3) 1.909(9), Re−C(1) 1.911(6), Re−C(2) 1.935(6), Re−N(1) 2.166(4), Re−N(2) 2.168(6), Re−Cl 2.4993(13), C(3)−Re−C(1) 85.0-(3), C(3)−Re−C(2) 90.1(4), C(1)−Re−C(2) 89.5(3), C(3)−Re−N(1) 96.9(4), C(1)−Re−N(1) 92.5(2), C(2)−Re−N(1) 172.9(6), C(3)−Re−N(2) 171.3(3), C(1)−Re−N(2) 98.6(2), C(2)−Re−N(2) 97.8(4), N(1)−Re−N(2) 75.1(3).

(1.29 V versus NHE),[28] the ruthenium-modified nucleoside **5** is a suitable candidate for ET measurements.

Diffraction quality crystals of **6** were obtained by slow diffusion of pentane into an anhydrous methanol solution (Figure 3). The complex crystallizes in the space group *Cc* with four molecules in the unit cell. The Ru−O bond lengths are 1.986−2.029 Å, O−Ru−O angles are 92.66 and 90.58°, close to those in $Ru(acac)_3$[29] and $Ru(tolyl\text{-}acac)_3$[30] (tolyl-acac = dibenzonate methane) (**2**) (Supporting Information), which shows that the replacement of one tolyl-acetylacetonate with an IMPy ligand does not perturb the $Ru(tolyl\text{-}acac)_3$ structure very much. The bond length of Ru−N bonds and bond angle of N(1)−Ru−N(2) are 2.02 Å and 80.59°, respectively.

Purification of High-Potential Ruthenium Nucleoside. 7 was prepared according to previous methods, and we determined further purification was necessary. A SP Sephadex C25 cation exchange resin was used with 0.05 M NaCl as eluent. A side product, **8** (Figure 1), was found to be present in about 30%. Crystals of the BF_4 salt of **8** were grown by slow diffusion of pentane into a dichloromethane solution. An ORTEP view of **8** is shown in Figure 4. The complex crystallizes in the space group $P2(1)/c$, with eight molecules in the cell. The Ru−N bond lengths are 2.037−2.059 Å, similar to Ru−N bond length of 2.056 Å in $[Ru(bpy)_3]^{2+}$.[31] The bond lengths of Ru−N bonds in the IMPy moiety are 2.050−2.086 Å, which are longer than those in bipyridine. This is consistent with an expected increase in bond length resulting from less π bonding in IMPy than that in bipyridine. Bond angles of N−Ru−N in bipyridine are 78.7−79.1°, close to 78.7° observed in $[Ru(bpy)_3]^{2+}$.[31] Bond angles of N−Ru−N in IMPy are 78.9° and 79.3°, respectively, which are consistent with those found in **6**.

The high yield of the side products **6** and **8** were investigated. We found that refluxing **4** in ethanol results in decomposition. TLC shows that multiple compounds appear within 4 h, and the mass spectrum shows peaks at 120.9, 226.9, and 353.1. These peaks correspond to the pyridine carboxamide, the thymidine fragment, and the sodium adduct of intact ligand **4**, and we conclude that this rearrangement is the source of **6** and **8**.

Chromatographic Separation and Characterization of Diastereomers of Ruthenium Nucleosides. The isolation of the diastereoisomers of **5** (*f* 1, $R_f = 0.18$; *f* 2, $R_f = 0.3$) was readily accomplished by column chromatography on silica with 4:1 dichloromethane/tetrahydrofuran. Λ**5** and Δ**5** (Figure 5) were isolated in 62 and 34%, respectively. The diastereoisomeric separation of **7** was achieved by cation-exchange chromatography on a SP Sephadex C25 support using 0.15M (-)-*O*,*O*′-dibenzoyl-L-tartrate as eluent. The diastereoisomers separated over a passage of 1∼1.5 m effective column length.[21,32−33] Isolated fractions were collected as the tartrate salts and converted to the hexafluorophosphate salts by metathesis. Λ**7** and Δ**7** (Figure 5) were obtained in 33 and 15%, respectively. The resolution of the individual diastereomers was confirmed by CD measurements. The CD spectra of Δ**7** and Λ**7** (Figure 6) resolved by this technique are in agreement with spectra reported previously for polypyridyl ruthenium(II) complexes.[21,34−36] The peaks near 300 nm were found to be characteristic of excitonic long-axis polarized $\pi-\pi^*$ transitions.[37] Cotton effects of the MLCT bands were found in the visible region.[37] The CD spectra of Δ**5** and Λ**5** (Figure 7) show the long-axis polarized transition due to the tolyl-acac ion at 280 nm. The MLCT band was found at 350 nm.[38]

Synthesis and Structural Characterization of Rhenium Nucleoside 9. 9 (Figure 1) was synthesized by stirring **4** with $Re(CO)_5Cl$ in refluxing THF under an inert atmosphere (Scheme 2). The compound was purified by column chro-

(28) (a) Shukla, L. I.; Adhikary, A.; Pazdro, R.; Becker, D.; Sevilla, M. D. *Nucleic Acids Res.* **2004**, *32* (22), 6565−6574. (b) Steenken, S.; Jovanovic, S. V. *J. Am. Chem. Soc.* **1997**, *119*, 617−618.
(29) Reynolds, P. A.; Cable, J. W.; Sobolev, A. N.; Figgis, B. N. *J. Chem. Soc., Dalton Trans.* **1998**, 559−569.
(30) Selected bond lengths (Å) and bond angles (deg) of $Ru(tolyl\text{-}acac)_3$ **2**: Ru−O(2) 1.984(3), Ru−O(4) 1.991(3), Ru−O(5) 1.998(3), Ru−O(3) 2.002(3), Ru−O(1) 2.010(3), Ru−O(6) 2.023(3), C(10)−O(2) 1.287(4), C(9)−C(10) 1.388(6), O(2)−Ru−O(4) 91.32(11), O(2)−Ru−O(3) 87.01(11), O(2)−Ru−O(1) 91.68(11), C(10)−O(2)−Ru 124.9(3), O(2)−C(10)−C(9) 124.2(4), C(8)−C(9)−C(10) 127.3(4), C(9)−C(10)−C(11) 120.9(4), C(12)−C(11)−C(10) 120.5(4), C(11)−C(12)−C(13) 121.4(5), C(14)−C(13)−C(12) 122.4(6), C(13)−C(14)−C(15) 123.7(6).
(31) Rillema, D. P.; Jones, D. S.; Levy, H. A. *J. Chem. Soc., Chem. Commun.* **1979**, 849−851.
(32) Fletcher, N. C.; Keene, F. R. *J. Chem. Soc., Dalton Trans.* **1999**, 683−689.
(33) Spillane, C. B.; Morgan, J. L.; Fletcher, N. C.; Collins, J. G.; Keene, F. R. *Dalton Trans.* **2006**, 3122−3133.
(34) Tzalis, D.; Tor, Y. *J. Am. Chem. Soc.* **1997**, *119*, 852−853.
(35) Rutherford, T. J.; Pellegrini, P. A.; Aldrich-Wright, J.; Junk, P. C.; Keene, F. R. *Eur. J. Inorg. Chem.* **1998**, 1677−1688.
(36) Fletcher, N. C.; Keene, F. R.; Viebrock, H.; Zelewsky, A. V. *Inorg. Chem.* **1997**, *36*, 1113−1121.
(37) Bosnich, B. *Inorg. Chem.* **1968**, *7(11)*, 2379−2386.
(38) Bosnich, B. *Acc. Chem. Res.* **1969**, *2(9)*, 266−273.

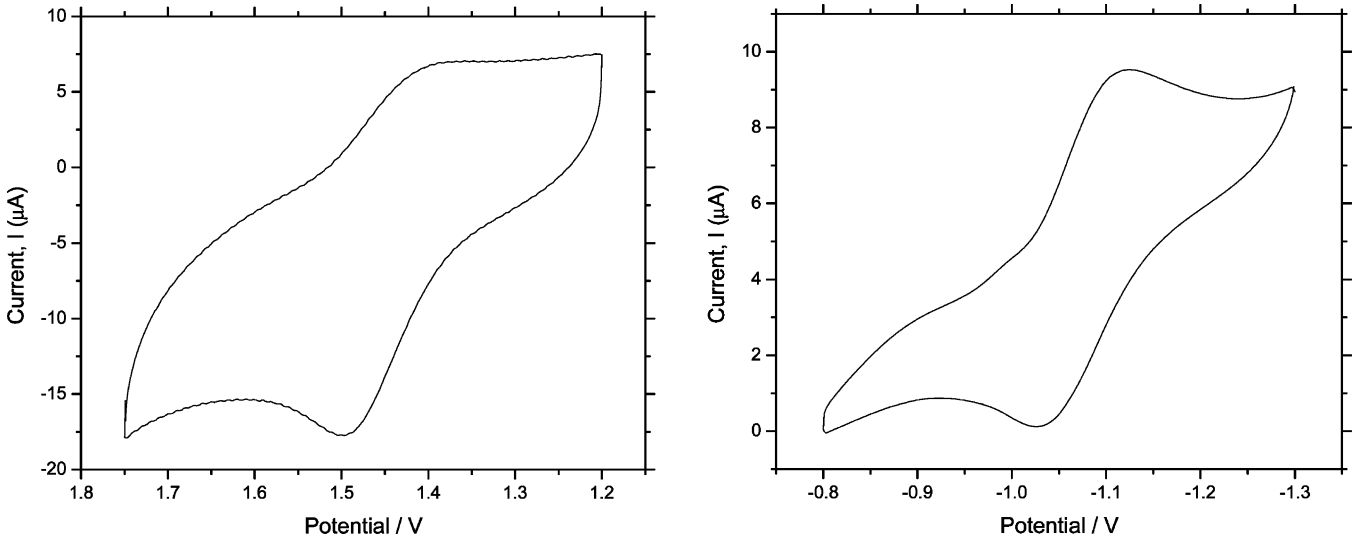

Figure 9. (a) Room-temperature cyclic voltammogram of **9** in 0.1 M ^{t}Bu$_4$PF$_6$/CH$_3$CN at a scan rate of 0.1 V/s, $E_{1/2}$ (ox) for **9** is 1.67 V versus NHE. (b) Room-temperature cyclic voltammogram of **9** in 0.1 M ^{t}Bu$_4$NPF$_6$/CH$_3$CN at a scan rate of 0.1 V/s, $E_{1/2}$ (red) for **9** is −0.81 V versus NHE.

matography, and diffraction quality crystals were isolated from slow vapor diffusion of heptane into acetone (Figure 8). The complex crystallizes in the space group *C*2, with four molecules in the unit cell. The C−C and C−O bond lengths for the ribose portion of **9** are very close to those of thymidine by itself as are the C−C, C−N, and C−O lengths for the purine ring.[39] There is some uncertainty in the refinement for C(10) due to disorder in the solvent molecules found in the crystals, but overall the structure shows very little perturbation of the thymidine base by the complexed rhenium ion.

Infrared spectroscopy of **9** in methylene chloride revealed five carbonyl stretches. The absorptions at 2025, 1925, and 1905 cm^{-1} were assigned to rhenium-bound carbonyls. These values are slightly higher in energy than the corresponding values for (bpy)Re(CO)$_3$Cl,[40] suggesting higher electron density on the metal center for **9**. Three peaks are expected due to the low symmetry of **9**. The broad absorption at 1712 cm^{-1} is assigned to both purine ring carbonyls, whereas the signal at 1693 cm^{-1} is assigned to the carbon−carbon double-band stretch between C15 and C16. These energies are only slightly different from reported values for solid thymidine (they differ by 3 and 12 cm^{-1} respectively),[41] most likely due to a combination of the solvation of the molecule and small changes in the bond lengths of the ring relative to the reported crystal structure of the unmodified nucleoside.

The electrochemistry of **9** was examined by cyclic voltammetry (Figure 9). A 1 mM solution of **9** in acetonitrile (0.1 M tetrabutyl ammonium hexafluorophosphate as the supporting electrolyte) showed complicated redox behavior, similar to other rhenium diimine tricarbonyl halide complexes.[42] Two reversible redox events were observed, where one quasi-reversible oxidation wave was assigned to rhenium(I) oxidation; $E_{1/2}$ = 1.67 V versus NHE (Table 2) compares well to $E_{1/2}$ = 1.67 V versus NHE for Re(CO)$_3$(bpy)Cl[42] and one reversible reduction wave; $E_{1/2}$ = −0.81 V versus NHE ($E_{1/2}$ = −1.11 V vs NHE for Re(CO)$_3$(bpy)Cl[42]) assigned to rhenium(I) reduction.

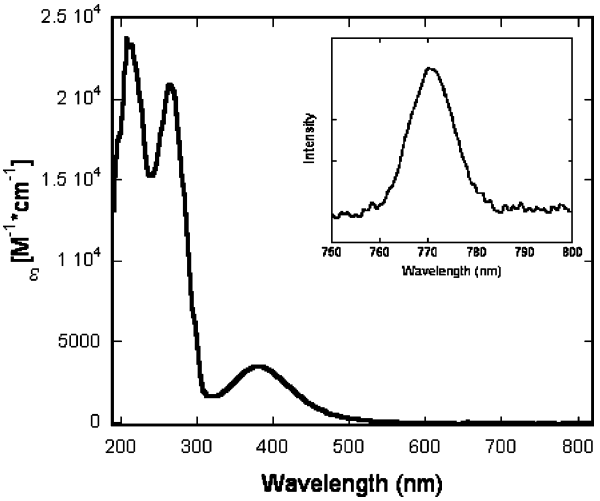

Figure 10. UV-vis absorption spectrum for **9** in 50 mM NaH_2PO_4/Na_2HPO_4, 75 mM NaCl buffer, pH 6.70. Inset: emission spectrum for **9** in 50 m M NaH_2PO_4/Na_2HPO_4, 75 mM NaCl buffer, pH 6.70; λ_{ex} = 355 nm.

Absorption and emission spectroscopy of **9** were obtained (Figure 10). The MLCT apparent at λ_{max} = 388 nm (ϵ = 3400 L mol^{-1}cm^{-1}) (Table 2) is nearly identical to the MLCT reported for (bpy)Re(CO)$_3$Cl,[43] suggesting that the rhenium-to-IMPy charge transfer is responsible for this absorption. Excitation of this MLCT at 355 nm in buffer leads to a relatively low-energy emission at λ_{max} = 770 nm. These spectral characteristics show little overlap with the reported guanine radical spectrum,[44] suggesting that transiently oxidized guanine bases might be spectroscopically

(39) Young, D. W.; Tollin, P.; Wilson, H. R. *Acta Crystallogr.* **1969**, *B25*, 1423−1432.
(40) Chen, P.; Palmer, R. A. *Appl. Spectrosc.* **1997**, *51*, 580−583.
(41) Mathlouthi, M.; Seuvre, A. M.; Koenig, J. L. *Carbohydr. Res.* **1984**, *134*, 23−38.
(42) Paolucci, F.; Marcaccio, M.; Paradisi, C.; Roffia, S.; Bignozzi, C. A.; Amatore, C. *J. Phys. Chem. B* **1998**, *102*, 4759−4769.
(43) Rossenaar, B. D.; Stufkens, D. J.; Vlcek, A. *Inorg. Chem.* **1996**, *35*, 2902−2909.
(44) Candeias, L. P.; Steenken, S. *J. Am. Chem. Soc.* **1993**, *115*, 2437−2440.

observed in a system employing **9** as a photo-oxidant. Time-resolved emission spectroscopy of this complex shows that the lifetime of the excited state is 17 ns.[45,46]

Conclusions

In conclusion, we have prepared a new donor−acceptor pair, ruthenium nucleoside **5** and rhenium nucleoside **9**, for ground-state ET studies in DNA. We improved the preparation of the high-potential ruthenium nucleoside **7** and isolated the diastereoisomers of **5** and **7**. CD measurements support the assignment of the absolute configuration. Further, we have structurally characterized a new high-potential rhenium nucleoside **9**. These nucleosides can be incorporated into oligonucleotides via the 5′ position of thymidine riboses. Given the oxidation potential of guanine,[28] **5**, **7**, and **9** are suitable candidates for electron donors and acceptors in ground-state DNA ET studies, and these studies are underway. Site-selective incorporation of these ruthenium and rhenium complexes on DNA enables us to measure the ground-state ET rates between the donor and acceptor.

(45) Low, D. W.; Winkler, J. R.; Gray, H. B. *J. Am. Chem. Soc.* **1996**, *118*, 117−120.
(46) Wan, C.; Fiebig, T.; Schiemann, O.; Barton, J. K.; Zewail, A. H. *Proc. Natl. Acad. Sci. U.S.A.* **2000**, *97*, 14052−14055.

Acknowledgment. We thank Dr. Deanna D'Alessandro at University of Sydney for helpful discussions and Dr. Danielle Gray for X-ray data collection and solving the crystal structure of **2**. We acknowledge the use of instruments in the Keck Biophysics Facility and financial support from the Nanoscale Science and Engineering Initiative of the National Science Foundation under the NSF Award Number EEC-0647560. We gratefully acknowledge support from the Center for Cancer Nanotechnology Excellence (CCNE) initiative of the National Institutes of Health's National Cancer Institute under Award U54CA119341.

Supporting Information Available: X-ray crystallographic files in CIF format for **2**, **6**, **8**, and **9** (CCDC 658536−658539); crystal data and molecular structure of **2**; IR spectrum for **9**; and mass spectrum of refluxing ligand **4** in ethanol. This material is available free of charge via the Internet at http://pubs.acs.org.

IC701250R